Phase Behavior of Ionic Microgels

D. Gottwald,[1,2] C. N. Likos,[2] G. Kahl,[1] and H. Löwen[2]

[1]*Center for Computational Materials Science and Institut für Theoretische Physik, Technische Universität Wien, Wiedner Hauptsraße 8-10, A-1040 Wien, Austria*

[2]*Institut für Theoretische Physik II, Heinrich-Heine-Universität Düsseldorf, Universitätsstraße 1, D-40225 Düsseldorf, Germany*

(Received 25 August 2003; published 9 February 2004)

We employ effective interaction potentials between spherical polyelectrolyte microgels in order to investigate theoretically the structure, thermodynamics, and phase behavior of ionic microgel solutions. Combining a genetic algorithm with accurate free energy calculations we are able to perform an unrestricted search of candidate crystal structures. Hexagonal, body-centered orthogonal, and trigonal crystals are found to be stable at high concentrations and charges of the microgels, accompanied by reentrant melting behavior and fluid-fcc-bcc transitions below the overlap concentration.

DOI: 10.1103/PhysRevLett.92.068301 PACS numbers: 82.70.–y, 61.20.–p, 64.70.–p, 83.80.Kn

Microgels are mesoscopically sized, covalently cross-linked polymer networks with diameters σ in the range between 10 nm and 1 μm. Most microgels are based on poly(*N*-isopropylacrylamide) (PNIPAM) or related copolymers that are cross-linked during emulsion polymerization, a process that can produce remarkably uniform particles [1,2]. Further, the preparation of microgels based on other materials, such as starch [3], has also been recently reported. When the polymer chains comprising the microgels carry ionic groups on their backbones, the latter dissociate upon solution into an aqueous solvent, leading to charged or *ionic* microgels [4–7]. Depending on the monomer concentration within their volume, microgels are further distinguished in *uniform* and *core-shell* ones [1], the latter consisting of a dense hard core and dangling, compressible chains at the outermost part of their corona [8].

A very useful concept in understanding the structure of soft matter systems is that of the effective interaction as a function of suitably chosen degrees of freedom of the mesoscopic particles constituting the system [9]. In our case, the effective pair potential, $v_{\rm eff}(r)$, is derived by holding the centers of mass of the microgels at fixed separation r and canonically integrating out the remaining degrees of freedom: for neutral microgels, the latter are the monomer coordinates and momenta, whereas for ionic ones the counterions have also to be traced out.

For *neutral*, dense microgel particles with a core-shell structure, several propositions for their effective interaction have been recently put forward [8,10,11], modeling the particles as hard spheres dressed with additional power-law interactions. In this Letter we turn our attention to the complementary case of ionic, uniform microgels that are loosely cross-linked and have low-monomer volume fractions $\phi \cong 0.5 \times 10^{-3}$ in their interior, a realistic value for charged PNIPAM particles [2]. Under such circumstances, the monomer and charge densities of the microgels can be approximated as being uniform [12]. Moreover, the steric contribution to their interaction is small, due to the low-monomer concentration, for values of the Flory parameter up to $\chi = \frac{1}{4}$ and thus it can also be ignored in comparison to the electrostatic energy and the counterion entropy [13]. The Hamaker constant H, which appears as an overall prefactor of the van der Waals attraction, scales with the monomer volume fraction as $H \sim \phi^2$ [14]; moreover, the strength of the dispersion attraction is further diminished by swelling [15]. Consequently, such attractions are weak and we ignore them as well. Finally, the elastic contributions to the interaction are caused by the deformations of the particles upon close approaches. Since we are dealing with loosely cross-linked microgels, we adopt the view, following Denton [7], that the microgels simply interpenetrate each other without being deformed; hence elastic terms can also be neglected. Therefore, the dominant contributions to the effective interaction arise—as it has been also explicitly demonstrated for the related physical system of polyelectrolyte stars [16]—from the electrostatic repulsion between the charged macromolecules, as well as from the confinement entropy of the counterions which additionally screen the bare electrostatic repulsion.

The effective potential $v_{\rm eff}(r)$ pertaining to the above-mentioned physical model has been recently worked out by Denton within the framework of the linear-response theory [7]. It takes the form $v_{\rm eff}(r) = v_{\rm mm}(r) + v_{\rm ind}(r)$, where $v_{\rm mm}(r)$ is the bare interaction between two uniformly charged spheres at center-to-center separation r and $v_{\rm ind}(r)$ is the part induced by the counterions. The latter reads in Fourier space as

$$\tilde{v}_{\rm ind}(k) = -\frac{36\pi Z^2 e^2}{\epsilon} \frac{\kappa^2}{k^6 a^4 (k^2+\kappa^2)} \left[\cos(ka) - \frac{\sin(ka)}{ka}\right]^2.$$

Here, Ze is the net microgel charge with the electron charge e, ϵ is the dielectric constant of the solvent, $a = \sigma/2$ is the particle radius, and $\kappa = \sqrt{4\pi n_c z^2 \lambda_{\rm B}}$ is the inverse Debye screening length from the counterions of density n_c and valency z. We will consider monovalent microions in what follows and then their density n_c is

related to the microgel density ρ via the electroneutrality condition $Z\rho = n_c$. Finally, $\lambda_B = e^2/(\epsilon k_B T)$ is the Bjerrum length, having the value $\lambda_B = 0.714$ nm for water at room temperature. (k_B denotes Boltzmann's constant and T the absolute temperature.) We have considered typical values of the microgel diameter σ ranging from 100 to 600 nm and macroion charges up to $600\,e$. The resulting total effective potential has an ultrasoft form, crossing over smoothly from a Yukawa potential at nonoverlapping distances ($r > \sigma$) to a slowly increasing repulsion for overlapping ones ($r < \sigma$) and remaining finite at the origin. There has been quite some interest in such unusual effective interactions recently, due to their relevance for polymeric colloids such as polyelectrolyte stars [16], star polymers [17], and polymer chains [18].

Based on this effective interaction, we have calculated the radial distribution function $g(r)$ and the structure factor $S(k) = 1 + \rho \int d^3r \exp[-i\mathbf{k}\cdot\mathbf{r}][g(r) - 1]$ of the fluid by employing the Rogers-Young (RY) closure [19] to the Ornstein-Zernike equation. This closure is designed to enforce consistency between the virial and compressibility routes via an adjustable parameter, if the pair potential is density independent. It is well known that the enforcement of thermodynamic consistency of the RY closure improves on the accuracy of the structural data. Here, however, we are dealing with an explicitly density-dependent interaction (through κ); in addition, the full free energy of the system includes volume terms that influence the total pressure [7,9]. Thus, the true pressure and compressibility of the system are not given by the standard formulas valid for density-independent pair potentials [20–22]. However, for a *given* thermodynamic point, the fluid has exactly the same structure with a fictitious one, which interacts via a *density-independent* potential identical to that of the *density-dependent* Hamiltonian. Therefore we can apply the RY closure in order to obtain $g(r)$ and $S(k)$ *alone*. For the thermodynamics of the fluid we have chosen a different route that holds for density-independent interactions: we solve the RY closure at every given density ρ of microgels for an array of scaled interaction potentials $\lambda v_{\mathrm{eff}}(r), 0 \le \lambda \le 1$, obtaining thereby the corresponding radial distribution functions $g^{(\lambda)}(r)$. Thereafter, the Helmholtz free energy of the system, $F_{\mathrm{ex}}(\rho)$, is calculated via the λ-integration route [23]. The full free energy of the fluid, $F_{\mathrm{fluid}}(\rho)$, is finally obtained as the sum $F_{\mathrm{fluid}}(\rho) = F_{\mathrm{id}}(\rho) + F_{\mathrm{ex}}(\rho) + F_{\mathrm{vol}}(\rho)$, with the ideal free energy $F_{\mathrm{id}}(\rho) = Nk_BT[\ln(\rho\sigma^3) - 1]$ and the extensive "volume terms" $F_{\mathrm{vol}}(\rho)$ resulting from integrating out the counterion degrees of freedom [24].

We found that the structure factor of ionic microgels displays anomalous behavior, akin to that seen for star polymers [25] and polyelectrolyte stars [26]: as the density increases up to the overlap concentration $\rho_*\sigma^3 \cong 1.5$, the height of the peak maximum grows and its position $k_{\max}$ scales as $\rho^{1/3}$. However, above the overlap concentration the position of the main peak becomes very insensitive to the density and its height diminishes, whereas it is now the second peak that starts growing. The reasons for this anomalous behavior lie in the crossover of the effective interaction from a Yukawa form, relevant for large separations and thus low densities, to a very soft one, which dominates at high concentrations. There, the weak repulsion is not capable of maintaining strong positional correlations within the fluid, leading thereby to a decrease in the height of the structural peak.

In order to draw the phase diagram of the system, we extended our investigations to crystal structures. To this end, we applied a novel genetic algorithm (GA) [27] which allows an unrestricted, parameter-free search of possible candidate structures. This GA can be viewed as an optimization strategy, using features of evolutionary processes as key elements to find the optimal solution for a problem [28]. In our application, the GA starts (for a given set of system parameters) from a population of individuals, each of them representing a possible crystal structure: an individual stands for a set of primitive vectors of a Bravais lattice in a coded form, and eventually it includes positions of further atoms in a nonsimple lattice. To be more specific, the individual is a string of so-called genes of fixed length where each gene can take the value 0 or 1; it is thus a binary representation of the lattice vectors. A population is formed by a large (but finite) number of individuals. The individuals are now evaluated by a positive fitness function f in the sense that a higher fitness value represents a better solution. We have chosen f to be proportional to $\exp(-F/F_e)$, F being the free energy of a given crystalline structure and $F_e = e^2/a$. In the first generation of population pairs of parents are chosen, triggered by their respective fitness value. Two new individuals of the next generation are created by cutting the parents' gene sequences at a randomly chosen point and cross-combining them. In addition, mutations are performed on these individuals with a probability $p_m = 0.001$ by flipping the value of one randomly chosen gene from 0 to 1 or vice versa. Thus the second generation of genes is created and we continue the cycle. Track is kept of the individual with the highest fitness value in each generation; the one with the absolutely highest fitness value is then refined in a steepest descent minimization and represents the stable crystal structure of the search. One particular problem we had to face and where special care had to be taken is related to the uniqueness of the representation of a specific structure: a given crystal structure can be represented by two equivalent sets of primitive vectors and thus by different individuals. 1000 individuals per generation and 100 iteration cycles were found to be largely sufficient for a good convergence of the algorithm. The power of this algorithm lies in the fact that it is able to *predict* in an unrestricted search equilibrium structures, while conventional methods that determine phase diagrams consider only equilibrium structures, which are taken from a preselected and limited number of crystal

candidates. The only restriction of the GA method is that this optimization process has to be performed separately for every class of lattices possessing a given number N_b of basis particles. We have considered lattices with $1 \leq N_b \leq 8$ [29].

We have applied the GA at $T = 0$; the calculation of the free energy F (and of the fitness function f) was done via lattice sums. The possible structures selected by the GA in this way are the face-centered cubic (fcc), the body-centered cubic (bcc), the simple hexagonal, the body-centered orthogonal (bco), and the simple trigonal. Only these five candidate structures were then considered for the determination of the full phase diagram for $T > 0$: for this step we have applied an Einstein model with Hamiltonian $\mathcal{H}_0$ (characterized by a spring constant) as a reference state for the true Hamiltonian $\mathcal{H}$. We made use of the Gibbs-Bogoliubov inequality, $F \leq F_0 + \langle \mathcal{H} - \mathcal{H}_0 \rangle_0$, where the free energy of the reference system is F_0: the minimum of the right-hand side with respect to the stiffness of the Einstein springs (and any additional free parameters, such as the size ratios and angles of the considered conventional unit cells) provides the lowest upper bound and thus a good approximate value for the free energy F. After having obtained the minimum value $F_{\min}(\rho)$ of F, the total free energy of the crystal, $F_{\text{solid}}(\rho)$, was obtained as $F_{\text{solid}}(\rho) = F_{\min}(\rho) + F_{\text{vol}}(\rho)$, to take into account the volume free energy $F_{\text{vol}}(\rho)$, as was done for the fluid. The phase boundaries were drawn through the common-tangent construction.

The resulting phase diagram for fixed particle size $\sigma = 100$ nm is shown in Fig. 1 on the charge-density plane. An unusual topology as well as a variety of crystalline phases results. At densities roughly below the overlap value ρ_*, the system freezes into the fcc lattice, which undergoes a

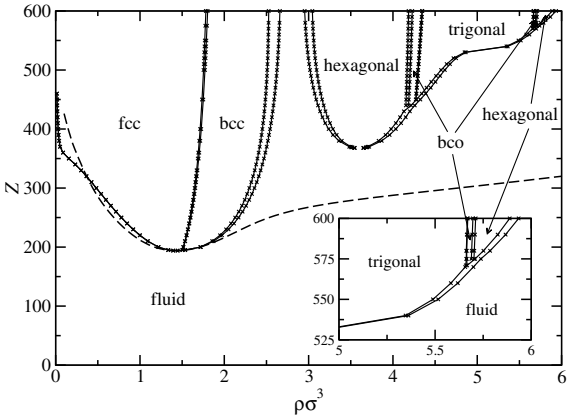

FIG. 1. The phase diagram of ionic microgels with diameter $\sigma = 100$ nm. The crosses denote calculated phase boundaries, whereas the lines are guides to the eye connecting these points. The unlabeled narrow regions between phases denote domains of phase coexistence (density jumps), whereas the dashed line is the locus of points in which the highest peak of $S(k)$ attains the Hansen-Verlet value 2.85. The inset shows the high-density, high-charge part in more detail.

structural phase transformation into a bcc structure at higher densities. This crystallization transition is typical for systems interacting by means of a screened Coulomb (Yukawa) interaction. Nevertheless, one unusual property of the system is that this crystallization takes place only if the charge Z exceeds a "critical value" $Z_c \cong 190$. For lower charges, the repulsion between the microgel colloids is too weak for any crystal to be sustained and thus the fluid is stable there for all concentrations [30]. Associated with the lack of crystallization for low values of Z is the reentrant melting scenario that sets in at higher charge values. The bcc solid remelts upon increasing the density, a feature seen also in star polymer solutions [31] and in the Gaussian core model [32]. For even higher densities ($\rho\sigma^3 \gtrsim 2.5$) a "fluid gap" first appears and thereafter the reentrant melting scenario repeats itself, but the stable crystal lattices are not cubic. Instead, the system crystallizes into unusual structures, such as the hexagonal, bco, and trigonal lattices. A topologically similar phase diagram has been obtained for a system of weakly charged polyelectrolyte chains using a completely different approach, based on a generalized Flory-Huggins theory in the weak segregation approximation [33].

The stability of exotic, highly anisotropic structures is a characteristic of ultrasoft interactions. In the case at hand, the traditional freezing interpretation by means of an effective hard-sphere diameter does not apply any more. The weak repulsions characteristic for close approaches make it possible that the system prefers, for energetic reasons, to assume configurations in which any particle is surrounded by a small number of neighbors at close distance, leaving successive neighboring shells farther apart. The energetic penalty for close interparticle approaches is not prohibitively large (as in the case of steep repulsions) and hence low-coordinated, anisotropic crystals can be stabilized. The unconventional character of the high-density freezing scenarios of the system is further corroborated by the violation there of two common structural criteria. First, as can be seen in Fig. 1, the Hansen-Verlet freezing criterion [34] does not hold along the second reentrant freezing lines, while it does so for the low-density side. Second, from the point of view of the crystal, the Lindemann criterion states that a solid melts when the ratio L of the root-mean-square displacement of a particle around its equilibrium position over the nearest neighbor distance exceeds a value of about 10%. We have calculated L for all crystal structures encountered in the phase diagram (Fig. 1), finding that at the high-density part of the phase diagram L is much higher, of the order of 20%. More importantly, it is *not* the crystal with the lowest value of L that wins; this would be—depending on density—the fcc or bcc lattice again. Instead, the crystal with the lowest L value *among the noncubic ones* turns out to be the most stable one.

We finally discuss the dependence of the phase behavior of the system on the particle diameter σ now for a *fixed*

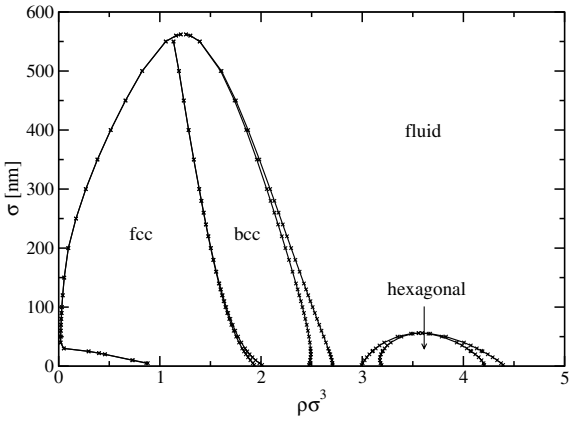

FIG. 2. The phase diagram of ionic microgels for fixed charge $Z = 300$ and varying particle diameter σ.

value of the charge Z, shown in Fig. 2. For sufficiently low values of σ, a succession of freezing and reentrant melting transitions is obtained, which are similar to the ones shown in Fig. 1. However, when the particles are large enough, neither the electrostatic interaction (which is now weak, since $\sigma \gg \lambda_B$) nor the entropic contributions from the counterions (which are also weak since the available volume for them to dissolve grows) are strong enough to stabilize a crystal and hence the system remains fluid at all concentrations.

In conclusion, we have calculated the phase diagram of loosely cross-linked, low-monomer ionic microgels as a function of the charge, concentration, and size of the particles: a host of unconventional lattices was found to be stable at high concentrations, accompanied by double-reentrant melting. Both the stabilization of exotic crystals by means of spherically symmetric interactions and the violation of the traditional melting and freezing criteria demonstrate that soft interactions offer an obviously unexpected rich variety of new physical phenomena and that the conventional views on crystallization gained from hard potentials have to be revisited thoroughly. The mechanisms bringing about these features are quite general for this class of interactions, a conclusion that is supported by the topological similarity of the phase diagram with that of star polymer solutions [31] and of polyelectrolyte stars [35]. It is anticipated that not only the equilibrium but also the dynamical behavior of ionic microgel solutions will be highly unusual [36], opening the way for a wealth of possibilities to manipulate the rheological behavior of microgel solutions that may lead to interesting applications, including the controlled fabrication of ordered lattices.

D. G. and G. K. acknowledge financial support by the FWF under Projects No. P15758-TPH and No. P14371-TPH. This work has been supported by the DFG through the SFB-TR6.

[1] R. Pelton, Adv. Colloid Interface Sci. **85**, 1 (2000).
[2] B. R. Saunders and B. Vincent, Adv. Colloid Interface Sci. **80**, 1 (1999).
[3] Y. Dziechciarek *et al.*, J. Colloid Interface Sci. **246**, 48 (2002).
[4] G. M. Eichenbaum *et al.*, Macromolecules **32**, 4867 (1999).
[5] A. Fernández-Nieves *et al.*, Macromolecules **33**, 2114 (2000).
[6] Y. Levin *et al.*, Phys. Rev. E **65**, 036143 (2002).
[7] A. R. Denton, Phys. Rev. E **67**, 011804 (2003).
[8] C. L. Berli and D. Quemada, Langmuir **16**, 10509 (2000).
[9] C. N. Likos, Phys. Rep. **348**, 267 (2001).
[10] A. Fernández-Nieves *et al.*, Langmuir **17**, 1841 (2001).
[11] J. Wu *et al.*, Phys. Rev. Lett. **90**, 048304 (2003).
[12] I. Varga *et al.*, J. Phys. Chem. B **105**, 9071 (2001).
[13] This estimate is based on a Flory-Huggins type of analysis, taking two uniform microgels at full overlap and demanding that the resulting steric repulsion, in good solvent conditions, is about 1 order of magnitude lower than the typical electrostatic and counterion contributions derived in Ref. [7].
[14] J. Wu *et al.*, Macromolecules **36**, 440 (2003).
[15] F. Gröhn and M. Antonietti, Macromolecules **33**, 5938 (2000).
[16] A. Jusufi *et al.*, Phys. Rev. Lett. **88**, 018301 (2002); J. Chem. Phys. **116**, 11011 (2002).
[17] C. N. Likos *et al.*, Phys. Rev. Lett. **80**, 4450 (1998).
[18] A. A. Louis *et al.*, Phys. Rev. Lett. **85**, 2522 (2000).
[19] F. J. Rogers and D. A. Young, Phys. Rev. A **30**, 999 (1984).
[20] A. A. Louis, J. Phys. Condens. Matter **14**, 9187 (2002).
[21] F. H. Stillinger *et al.*, J. Chem. Phys. **117**, 288 (2002).
[22] J.-P. Hansen and I. R. McDonald, *Theory of Simple Liquids* (Academic, New York, 1986), 2nd ed.
[23] C. F. Tejero and M. Baus, J. Chem. Phys. **118**, 892 (2003).
[24] R. van Roij *et al.*, Phys. Rev. E **59**, 2010 (1999).
[25] M. Watzlawek *et al.*, J. Phys. Condens. Matter **10**, 8189 (1998).
[26] H. Löwen *et al.*, J. Phys. A **36**, 5827 (2003).
[27] D. Gottwald *et al.* (to be published).
[28] D. E. Goldbert, *Genetic Algorithms in Search, Optimization, and Machine Learning* (Addison-Wesley, Reading, MA, 1989).
[29] We restricted our search to periodic structures only. Glassy states are in general metastable; they could nevertheless be approximated by superlattices with a large number of basis vectors. Our approach did not yield any tendency of the system to crystallize into structures with a large number of basis vectors.
[30] In our case, the volume terms are convex, in distinction to the case of Ref. [24].
[31] M. Watzlawek *et al.*, Phys. Rev. Lett. **82**, 5289 (1999).
[32] A. Lang *et al.*, J. Phys. Condens. Matter **12**, 5087 (2000).
[33] E. E. Dormidontova *et al.*, Macromol. Theory Simul. **3**, 661 (1994).
[34] J.-P. Hansen and L. Verlet, Phys. Rev. **184**, 151 (1969).
[35] N. Hoffmann *et al.* (to be published).
[36] G. Foffi *et al.*, Phys. Rev. Lett. **90**, 238301 (2003).